Research Article | Vol. 12, No. 4 / 1 April 2021 / Biomedical Optics Express 1962
Biomedical Optics EXPRESS

Investigating tunneling nanotubes in ovarian cancer based on two-photon excitation FLIM-FRET

SHIQI WANG, YANPING LI, YIHUA ZHAO, FANGRUI LIN, JUNLE QU, AND LIWEI LIU*

Key Laboratory of Optoelectronic Devices and Systems of Guangdong Province & Ministry of Education, College of Physics and Optoelectronic Engineering, Shenzhen University, Shenzhen, Guangdong Province 518060, China
liulw@szu.edu.cn

Abstract: Precise and efficient cell-to-cell communication is critical to the growth and differentiation of organisms, the formation of various organism, the maintenance of tissue function and the coordination of their various physiological activities, especially to the growth and invasion of cancer cells. Tunneling nanotubes (TNTs) were discovered as a new method of cell-to-cell communication in many cell lines. In this paper, we investigated TNTs-like structures in ovarian cancer cells and proved their elements by fluorescent staining, which showed that TNTs are comprised of natural lipid bilayers with microtubules as the skeleton that can transmit ions and organelles between adjacent cells. We then used fluorescence resonance energy transfer (FRET) based on two-photon excitation fluorescence lifetime imaging microscopy (FLIM) (TP-FLIM-FRET) to detect material transport in TNTs. The experimental results showed that the number of TNTs have an impact on the drug treatment of cancer cells, which provided a new perspective for TNTs involvement in cancer treatment. Our results also showed that TP-FLIM-FRET would potentially become a new optical method for TNTs study.

1. Introduction

Intercellular communication has proven to be involved in many important physiological activities in cancer growth and metastasis [1,2]. There are many communication methods between cancer cells, such as exosomes, secreted microRNAs, and gap junction [3–5]. More than a decade ago, tunneling nanotubes (TNTs) were discovered as a new method for cell-to-cell communication. TNTs were first found in cultured rat pheochromocytoma PC12 cells in 2004 [6], and later on was found in many cell lines, such as rat primary neurons, astrocytes, and immune cells [7,8]. TNTs have been defined as thin(50–1000 nm in width), long-range F-actin-based membrane nanotubes which mediates intercellular communication between linked cells by directly participating in the process of substances transfer, such as mitochondria, microRNAs, immunodeficiency virus [9–11].

In previous research, correlative light-electron microscopy, electron tomography and confocal microscopy were usually used to image the structure of TNTs and monitor the material transfer process [12]. However, the spatial resolution of these microscopy techniques is limited and cannot directly detect the interactions between proteins in TNTs. Fluorescence resonance energy transfer (FRET) happens only when the distance between the donor and acceptor fluorescent molecules is less than 10 nm. Due to its spatial resolution at nanometer scale, FRET became an important optical method to study the biological processes in living cells [13]. Compared with other conventional FRET technologies, such as: spectral FRET, sensitized emission FRET and acceptor photobleaching FRET [14–16]. Fluorescence lifetime imaging microscopy (FLIM) based FRET is a unique method, which relies on the measurement and 2D mapping of fluorescence lifetime of

#418778 https://doi.org/10.1364/BOE.418778
Journal © 2021 Received 11 Jan 2021; revised 25 Feb 2021; accepted 25 Feb 2021; published 9 Mar 2021

Biomedical Optics EXPRESS

donor molecules [17]. Fluorescence lifetime imaging is an effective quantitative tool and not affected by changes in the laser light intensity, therefore it can be used to measure the intracellular microenvironment [18]. In our study, FRET that is based on two-photon (TP) excitation FLIM (TP-FLIM-FRET) provides a new imaging technique to characterize the transport of substances in TNTs.

Owing to the important role of TNTs in intercellular communication, there has been an increasing interest in the investigation TNTs in pathogenesis of various diseases, such as metastasis of cancer or in immunological processes [8]. Desir, S. et al. found that the increase in the number of TNTs in cells is dose-dependent fashion of Doxorubicin. Further tests showed that TNTs formation was upregulated in aggressive forms of pancreatic carcinoma and acted as a novel method for drug efflux. Besides, they have found TNTs, which connecting an island of malignant pancreatic cells to another group of cells at long-range, in resected pancreatic adenocarcinoma stained with Hematoxylin and Eosin (H&E) [19]. Kolba MD' s studies found that transmission of vesicles via TNTs from stromal cells increases resistance of leukemic cells to the tyrosine kinase inhibitor [12]. The disruption of TNTs has been found to sensitize prostate cancer (pCa) to treatment-induced cell death [20]. In sum, TNTs have been found in tissue sections and cells, and proven to have an impact on the results of drug treatments. In this study, we proved the role of TNTs in drug therapy and explored the potential effect of TNTs in cancer treatment.

2. Materials and methods

2.1. Reagents

The following dyes were purchased from YEASEN (shanghai, China): DiO(DiIC18(3)), Cell Counting Kit (CCK-8). The following dyes were purchased from Maokangbio (shanghai, China): SBFI AM (Na^+ Indicator), PBFI AM (K^+ Indicator). The following dyes were purchased from MedChemExpress: 1-Heptanal, Meclofenamic Acid. The following dyes were purchased from Thermo Fisher Scientific: LysoTracker Green DND-26, MitoTracker Green FM, Fluo-4,AM,Cell Permeant, Connexin 43 Monoclonal Antibody (CX-1B1), Alexa Fluor 488 donkey anti-rat IgG(H + L), 4% Paraformaldehyde Fix Solution, alpha Tubulin Monoclonal Antibody (236-10501), Actin Monoclonal Antibody (mAbGEa). The following dyes were purchased from Beyotime: 0.1% Triton X-100 Solution, Blocking Solution, QuickBlock Primary Antibody Dilution Buffer for Western Blot, QuickBlock Secondary Antibody Dilution Buffer for Western Blot, Immunol Staining Wash Buffer, and Annexin/PI. CX43-EGFP and CX43-mCherry were customized from VectorBuilder, Guangzhou, China. Their restriction maps were shown in Fig. S1. Paclitaxel (>98.0%(HPLC)) was purchased from Tokyo Chemical Industry (TCI).

2.2. Cell culture

Human ovarian cancer cells OVCAR-3 (ATCC, Manassas, USA) were cultured in DMEM (Dulbecco's Modified Eagle medium) supplemented with 10% fetal bovine serum (FBS) and 1% antibiotic-antimycotic solution (Gibco, Invitrogen, NY, USA) at 37°C in a humidified 5% CO_2 incubator.

2.3. Immunofluorescence Staining

Immunofluorescent staining was performed to study the expression of CX43. Cells were cultured overnight to achieve appropriate density (60-80%). Cells were fixed with 4% Paraformaldehyde Fix Solution for 15 min at room temperature and then gently washed with PBS. After treated with blocking solution, Cells were permeabilized with 0.1% Triton X-100 Solution at room temperature for 30 min. 5 µg Connexin 43 Monoclonal Antibody (CX-1B1) were diluted in 1 mL QuickBlock Primary Antibody Dilution Buffer. Incubate overnight at 4°C. 5 µL Alexa FluorTM 488 donkey anti-rat IgG(H + L) were diluted in 1 mL QuickBlock Secondary Antibody Dilution

Biomedical Optics EXPRESS

Buffer. Sample was protected from light and incubate for 1 hour at room temperature. Finally, the cells were washed 3 times with PBS. Simple was imaged under Confocal microscopy at 60x with the 525/50 filter.

2.4. Plasmid transfection

Cells were plated onto glass bottom cell culture dishes (Φ20 mm) at 1×10^5 cells/well 24 h. Dilute 4 µL Lipofectamine 2000 Reagent and 4 µL Cx43-EGFP (or Cx43-mCherry) DNA in 200 µL DMEM respectively. Add diluted DNA in diluted Lipofectamine 2000 Reagent (1: 1 ratio). Incubate for 20 min at room temperature. Add DNA-lipid complex to cells. Incubate overnight at 37°C. Gently wash the cells 3 times in PBS (5 min/wash) before image.

2.5. Imaging

Cells were plated onto glass bottom cell culture dishes (Φ20 mm) at 1×10^5 cells/well 24 h prior to image. Cells were incubated with the Ca^{2+} indicator Fluo-4 (3 µM) at 37°C for 30 min. Unloaded Fluo-4 was removed by three washes with PBS. Finally, we added 1 mL of PBS to the cell culture dish. Single-photon imaging of live cells was performed using a confocal microscope (A1R MP+, Nikon) equipped with four CW lasers: 405, 488, 561 and 640 nm. The corresponding four detection channels were separated by a series of long pass (LP), dichroic mirrors and bandpass (BP) filters: (1) LP (reflect) 495 nm and BP 450/50 nm; (2) LP (reflect) 560 nm and BP 525/50 nm; (3) LP (reflect) 640 nm and BP 595/50 nm; (4) LP (transmit) 640 nm and BP 700/75 nm. Laser power and detector gain were set to levels just below the saturation of the detector for each dye. Using confocal system, the image resolution was 1024×1024 pixel, the scanning speed was 0.08 µm/px, and the laser power was around 1 mW (Fig. 1(a-g), and Fig. 3(a)). The image resolution was 512×512 pixel, the scanning speed was 0.25 µm/px (Fig. 1(h-n), and Fig. 3(b-c)). The two-photon experiments were performed by a femtosecond laser with a pulse width of 100 femtosecond and repetition rate of 80 MHz (Chameleon Discovery, Coherent). Using TP-FLIM-FRET system, 960 nm and 1100 nm laser were used to stimulate antibody-expressed cells, the power range of laser was 5-7 mW (Fig. 3(b-c)).

2.6. Cell viability assays

The cell viability of cultured cells was quantified using a Cell Counting Kit (CCK-8) (Dojindo Molecular Technologies). OVCAR-3 cells were seeded onto 96-well plates. After incubated at room temperature for 24 h, cells were treated with Paclitaxel, 1-heptanal, and Meclofenamic Acid respectively. In experimental groups A-B and D-F, the concentration gradients of 1-heptanal and Meclofenamic Acid were 0, 0.5, 1, 2, 4, 6 µM. In experimental group C, the concentration gradients of Paclitaxel were 0, 0.5, 1, 2, 4, 6 µM. In experimental groups D-F, the concentration of Paclitaxel was 4 µM. After another 24 h of incubation, CCK-8 solution is added to 96-well plates. Incubate at room temperature for 2 h, Various shades of orange, which represented the amount of living cells, were measured with the CCK-8 cell counting kit, and the absorbance at 450 nm was measured with a microplate reader (RT-6100, Tayto) to calculate the cell viability.

2.7. Statistical analysis

The significance of the variability among groups was analyzed with GraphPad Prism 7.0 software (GraphPad, La Jolla, CA, USA) using hot map. Differences were considered to be statistically significant if $p < 0.1$.

Biomedical Optics EXPRESS

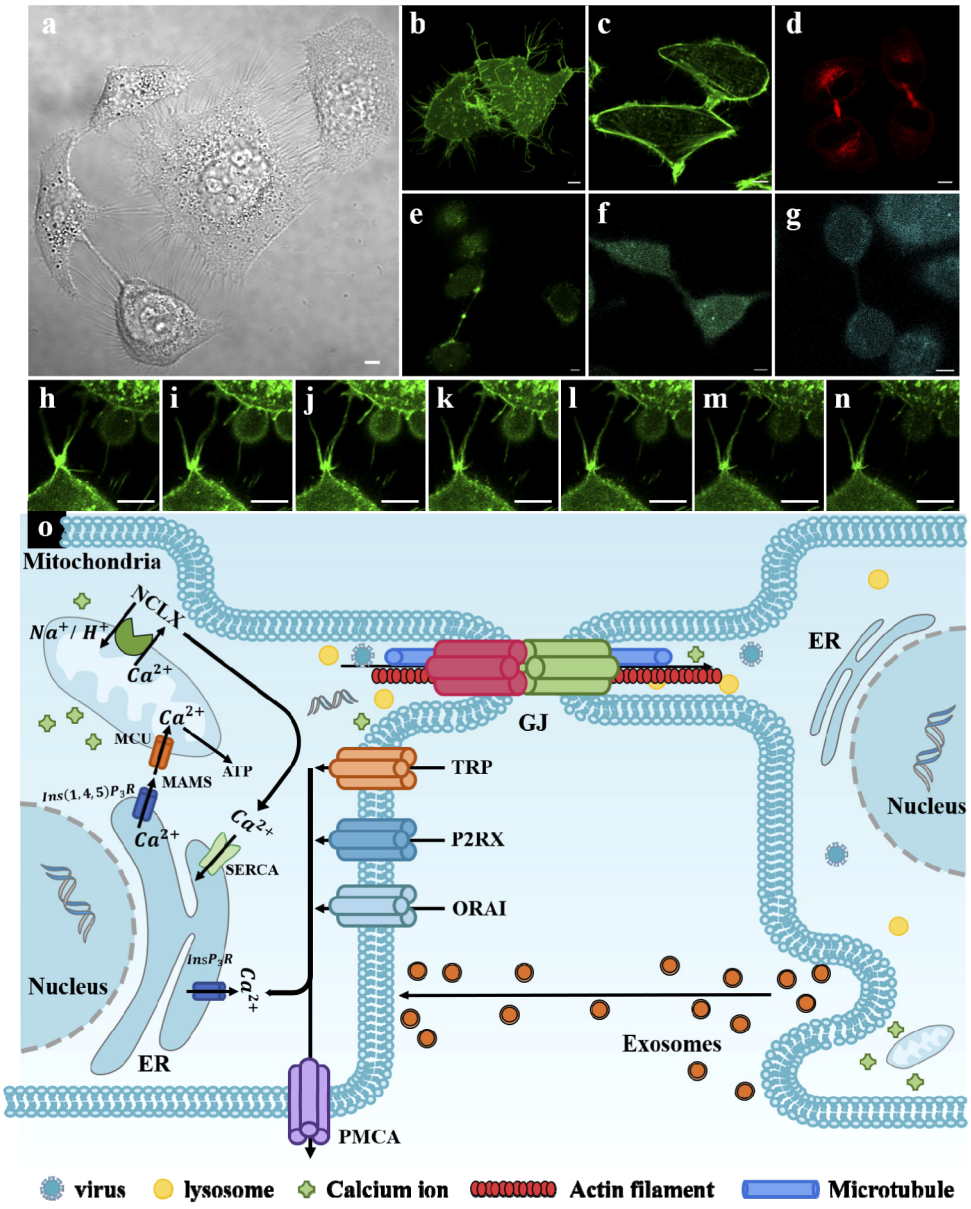

Fig. 1. TNTs are identified in human ovarian cancer. (a)Tunneling nanotube-like structures, likely TNTs, were visualized in OVCAR3 cell networks. (b) The outermost surface of TNTs is made up of phospholipid bilayer. (c, d) TNTs contain both actin and microtubules inside. (e-g) Ca^{2+}, Na^+ and K^+ ions have been proven to be transmitted through TNTs. (h-n) The heads of the filopodia of two adjacent cells contact to form TNTs. (o) A model of TNTs structure between adjacent cells. The scale bar in (a) indicates 5 μm, those in (b-g) indicate 10 μm, while those in (h-m) indicate 20 μm.

Biomedical Optics EXPRESS

3. Results

3.1. TNTs in ovarian cancer cells and their characteristics

Using OVCAR3 cells, a cell line of human ovarian cancer, we have previously found the TNTs-like connections between adjacent cells. We have determined that these structures are suspended between two adjacent cells and vary greatly both in lengths and diameters. The length of these structures ranges from 5 to 60 μm, and the diameter varies from 0.51 to 2 μm.

We used Confocal systems to imaging cells, which were incubated with a series of fluorescent probes to mark TNTs-like membrane structures, via a 60× oilimmersion objective. Using DiO (EX/EM=484/501), a probe for cell membrane, we found that TNTs-like structures are made up of lipid bilayer and are continuation of the cell membrane. After antibody staining, we found that TNTs contain actin filaments and microfilaments. Fluo-4, AM (Ex/Em=494/516), SBFI AM Na+ Indicator (Ex/Em = 380/500), and PBFI AM K+ Indicator (Ex/Em = 380/500) were used to incubate cells, as shown in Fig. 1(e-g), which proved that Ca2+, Na+ and K+ ions can be transported through TNTs. As the second messenger in cells, calcium ions participate in many physiological activities of cells and are extremely important for maintaining various metabolic processes in cells. In our previous research, the rapidly growing calcium ions in one cell can be transferred to adjacent cells via TNTs [21]. This reminds us that TNTs play an important role in calcium wave transmission between cells. As shown in Visualization 1, Lysosome can also be transmitted between two neighboring cells through these structures. Overall, these data proved that these tube-like structures are TNTs.

There are mainly two patterns determining how TNTs are formed: (1) TNTs formation starts when the cells move apart after a tight contact [22,23]. (2) TNTs are the protrusions of a cell mediated by actin that continuously extends to adjacent cells [24]. To further study the formation process of TNTs, we incubated the OVCAR3 with calcium ion indicator and photographed the time series using a confocal microscope. As shown in Fig. 1(h-n) and Visualization 2, the heads of the two labeled filopodia touch to form TNTs. In addition, TNTs cross from one cell to another always choose the nearest distance. Our research provided a new pattern for the formation of TNTs.

Over the last decade, scientific research has effectively increased our understanding of the structures of TNTs and their formation mechanisms. Sartori-Rupp, A et al. found that TNTs are composed of a bundle of individual tunneling nanotubes (iTNTs) that filled with parallel actin bundles on which different membrane-bound compartments and mitochondria appear to transfer. They claimed that neuronal TNTs have distinct structural features compared with other cell protrusions [25]. But our experimental results proved that TNTs can be formed by filopodia connection in ovarian cancer cells. This is the biggest difficulty in TNTs research that these structures in different cell lines can be formed in diverse patterns and have different constituent elements. We suspect that the difference in TNTs may be related to cell specificity, and this problem might be solved from the perspective of genetic regulation.

As shown in Fig. 1(o), we propose a model of TNTs structures. We used phospholipid bilayers to simulate cell membranes. Combine our staining results and other researchers' studies on TNTs. We described TNTs as tubular structures composed of microfilaments and microtubules, surrounded by phospholipid bilayers. Mitochondria, lysosomes, viruses, and ions can be transmitted between two adjacent cells through TNTs. In particular, the instantaneous increase in Ca^{2+} concentration caused by laser light can also be transmitted between cells through TNTs [26,27].

3.2. Monitor the transmission of substances in TNTs using TP-FLIM-FRET

Among the traditional imaging technologies of TNTs, electron microscopy (EM) is often used. Because of its complicated operation (need to embed cells from the wall of the culture dish),

Biomedical Optics EXPRESS

it is not an ideal imaging technique. Anna Sartori-Rupp et al. adopted correlative FIB-SEM, light- and cryo-electron microscopy approaches to elucidate the ultrastructure organization of neuronal TNTs. Although the ultrastructure of TNTs can be imaged, damage to TNTs during the operation is still unavoidable and real-time imaging of material transmission is impossible. Using confocal microscopy and fluorescent dyes, the material transport in TNTs can also be observed. However, due to the limitation of confocal resolution (200 nm). The transmission of proteins in TNTs cannot be detected by traditional imaging techniques. In order not to damage the sample and realize the observation of intracellular protein transmission, we propose to use two-photon (TP) excitation FLIM (TP-FLIM-FRET) as a new detection method for TNTs.

The efficiency of FRET is closely related to the spatial distance between the donor and acceptor molecules and occurs only when the emission spectrum of donor overlaps with the excitation spectrum of receptor, and spatial distance between the donor and acceptor is less than 10 microns. As the distance increases, FRET decreases significantly. It is precisely because of this property that FRET is widely used in real-time detection of interaction between protein molecules, molecule movement and changes in intracellular calcium concentration [28,29]. The efficiency of FRET between the donor and acceptor can be expressed as:

$$E = \left(1 - \frac{\tau_{DA}}{\tau_D}\right) \times 100\% \tag{1}$$

where τ_{DA}nd τ_D represents the donor lifetime in the absence and presence of the acceptor. As it is not affected by Intracellular microenvironment and the intensity of the excitation light, FLIM becomes an ideal method to characterize the efficiency of FRET [30].

As shown in Fig. 2, TP-FLIM-FRET is implemented by combining a two-photon excitation laser scanning confocal microscope with a time-correlated single photon counting (TCSPC) module for lifetime measurement. The confocal microscope has high spatial resolution, 3D reconstruction and dynamic analysis functions. The light source of the two-photon excitation fluorescence lifetime imaging is an ultra-fast mode-locked Ti: sapphire laser delivering femtosecond laser in the near infrared region, which allows for low scattering and localized excitation. The advantages of this method include low photobleaching and phototoxicity, deeper tissue penetration, subcellular level resolution, and inherent tomographic capability [31]. Two-photon excitation fluorescence imaging is the method of choice for in vivo imaging. Time-correlated single photon counting (TCSPC) is a classic time-domain FLIM technology with ideal photon counting rate and high time resolution. TP-FLIM-FRET can perform high-resolution detection of living cells, observe the transmission of organelles in TNTs and detect FRET by TCSPC-FLIM.

In this study, we proved the possibility of TP-FLIM-FRET as a technical means for studying TNTs. In previous studies, Gap junctions (GJ) have been proven to exist in TNTs and is an important factor in the formation of TNTs. Gap junctions (GJ) are specialized cell membrane structures between adjacent cells and are a kind of channels that directly connect cells, which plays an important role in the coordination between cells and multicellular organs and the body's self-stabilization control [32]. X. Wang et al. found that only one end of the TNTs displayed membrane continuity, whereas the other exhibited a membrane border, which was immune-positive for Cx43 [33]. Patch-clamp analysis revealed that the TNTs conductance was voltage-sensitive, which has been identified as a characteristic feature of Cx43-containing gap junctions [34]. Furthermore, the gap junction blocker meclofenamic acid led to a reduction of the TNTs-dependent coupling [35]. Therefore, the TNTs connection is most likely formed by the GJ connection regulated by CX43. GJ can appear in different positions of TNTs, which is in line with our conjecture about the formation process of TNTs. As shown in Fig. 3(a), we incubated OVCAR3 with CX43 antibody and found that CX43 are distributed in the TNTs structures.

For further experiment, we designed two over-expression CX43 plasmids, CX43-EGFP and CX43-mCherry. EGFP-mCherry is a classic FRET pair and shows ideal properties for FLIM

Biomedical Optics EXPRESS

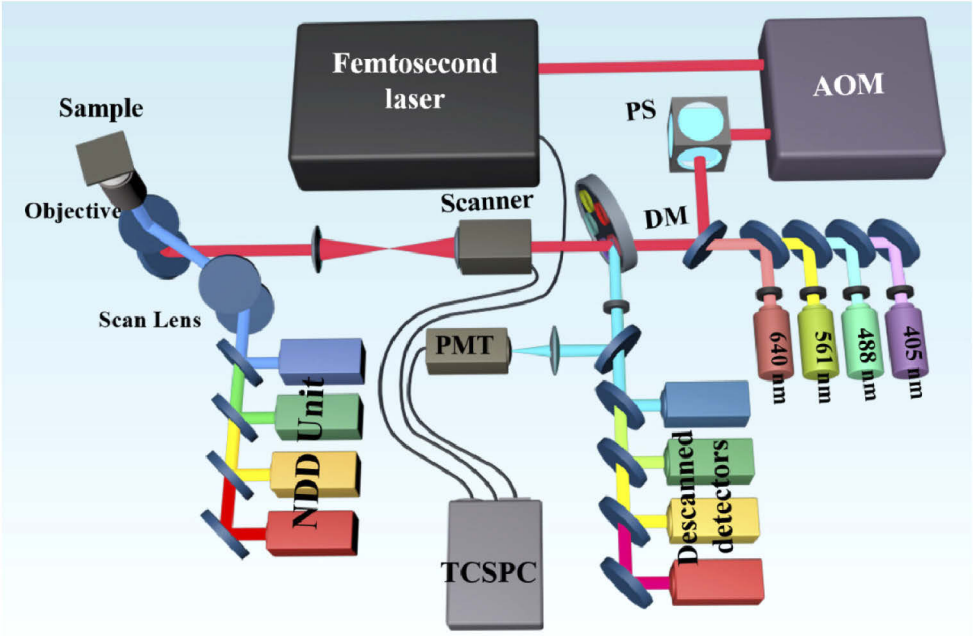

Fig. 2. The optical path diagram of TP-FLIM-FRET system.

detection of FRET and yields high accuracy both in vitro and in vivo. OVCAR3 cells were transfected with CX43-EGFP, as shown in Fig. 3. Then, using TP-FLIM-FRET to detect the donor's fluorescence lifetime in TNTs. Then, we separately transfected OVCAR3 cells with CX43-EGFP and CX43-mCherry for 24 hours. After the fluorescent protein is expressed in the cells, we inoculate two batches of cells in same cell dish. The cells will culture in the new dish for 24 h and regenerate TNTs. After that, we imaged the cells by TP-FLIM-FRET. FRET occurs in the TNTs of two connected cells, one cell is transfected with CX43-EGFP and the other cell is transfected with CX43-mCherry.

The fluorescence lifetimes were detected by TP-FLIM-FRET in the donor channel and the fluorescence decay curve was fitted by exponential model to estimate its corresponding fluorescence lifetime. The equation is given as follows:

$$I(\mathrm{t}) = \sum_{i=1}^{n} \alpha_i \exp\left(\frac{-t}{\tau_i}\right) \tag{2}$$

Here, $I(t)$ is the fluorescence intensity at time t; τ_i, $\propto_i$ is the fluorescence lifetime and contribution of each component, respectively.

The results are shown in Fig. 3, Fig. 4 and Table 1. The bi-component fluorescence lifetime of OVCAR3 transfected with only-donor were 1. 9 and 3.1 ns while cells transfected with FRET pair were 1.5 and 2.5 ns respectively. It can be seen from the figure that after the FRET effect occurs, the mean fluorescence lifetime become a shorter lifetime. As shown in Fig. 4, the lifetime spectrum obviously shifted to a shorter direction. FRET was happened and its energy transfer efficiency (E) was 16%. Two points were selected randomly from Donor-expressed cells and FRET Pairs-expressed cells. Then, using SPCImage to fit their fluorescence lifetime decay curve, as shown in Fig. S3.

The structure of TNTs is particularly fragile. Physical damage and long-term light stimulation will damage it. The classic image technologies for determining the structure of TNTs are severely

Biomedical Optics EXPRESS

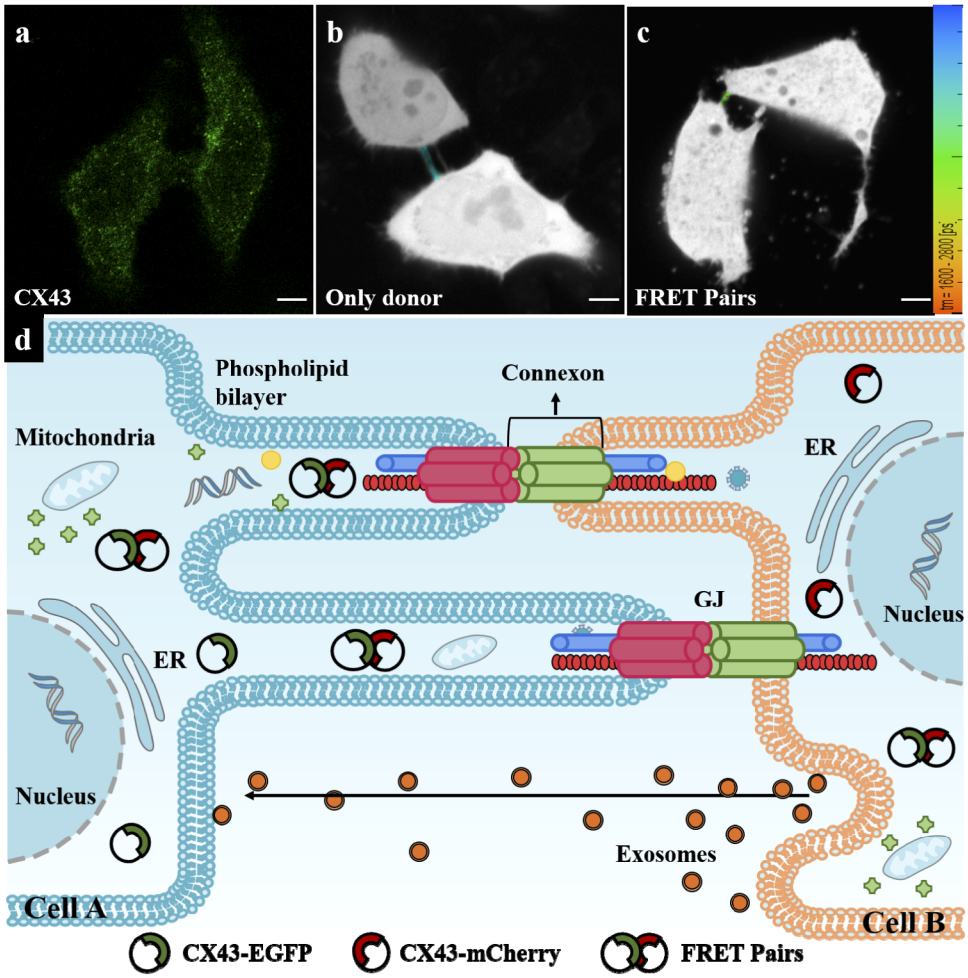

Fig. 3. Monitor the transmission of substances in TNTs using TP-FLIM-FRET. (a) OVCAR3 cells were incubated with Cx43 antibody. (b) OVCAR3 cells were transfected with overexpress Cx43-EGFP plasmid efficiently and fluorescence lifetime of TNTs was detected by TP-FLIM-FRET. (c) FRET occurs in the TNTs. (d) OVCAR3 cell A and B was transfected with CX43-EGFP respectively. The donor and recipient met through TNTs and caused FRET. The scale bar in (a-c) indicates 10 μm.

Table 1. Fluorescence lifetimes recovered from MLE analysis of time-resolved fluorescence of only-donor and FRET pairs.

	τ_1 (ns)	α_1 %	τ_2 (ns)	τ_m (ns)
Only-donor	1.9	51.94	3.1	2.5
FRET pairs	**1.5**	**40.39**	**2.5**	**2.1**

Biomedical Optics EXPRESS

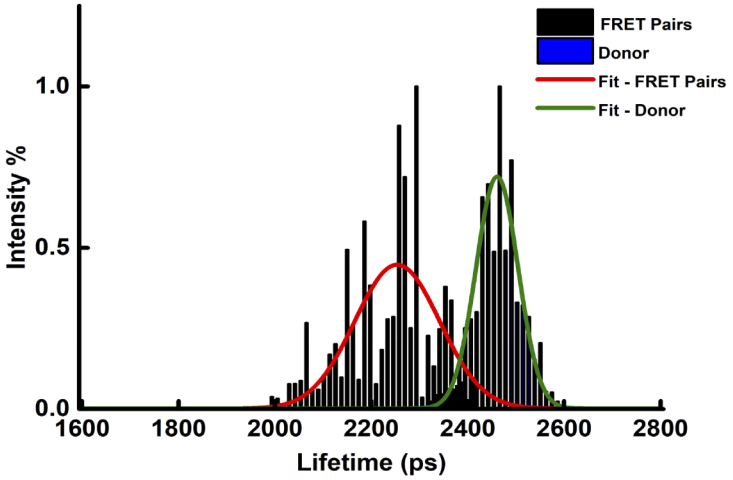

Fig. 4. The lifetime histogram of Donor-expressed cells and FRET Pairs-expressed cells.

limited for several reasons. The drawbacks of EM are its low-resolution and TNTs are easily broken. Our study showed that TP-FLIM-FRET offers an approach that can detect molecule movement in TNTs. Staining cells with plasmid provide a useful way targeting the protein of interest. Combined with TP-FLIM-FRET technology, it is possible to detect the action of the protein in TNTs.

3.3. Role of TNTs in the treatment of ovarian cancer cells

Many studies have shown that TNTs are involved in different processes such as stem cell differentiation, tissue regeneration, immune response, and cancer metastasis [8,36–39]. It has been found that in vitro TNTs formation and TNTs-mediated intercellular communication are significantly higher in several pathologic forms of disease, including virus infection, cancer, Chronic myeloid leukemia (CML) as well as tauopathies, and neurodegenerative diseases [11,40–44].The role of TNTs in these processes and these diseases is still under active investigation.

As one of the most common ovarian cancer chemotherapy drugs, paclitaxel can inhibit the depolymerization of microtubules, regulate the metaphase of mitosis and inhibit the progress of mitosis. It has been proved the GJ channels have been observed in TNTs [45].To explore the role of TNTs in drug treatment of ovarian cancer, we used gap junction blockers (1-heptanol and Meclofenamic Acid) to regulate the number of TNTs in the cells. Paclitaxel and 1-heptanol (or Meclofenamic acid) were used together to incubate OVCAR3.

As shown in Fig. 5, we have set up a total of six experimental groups. Concentration gradient 1-6 represent the different concentrations of working fluid. In particular, when the density gradient is 1, OVCAR3 cells were incubated with only PBS. It can be seen that the cell survival rate is close to 1. In experimental groups A-B, 1-heptanol and Meclofenamic Acid were added to OVCAR3 cells respectively. In team C, cells were cultured with different concentrations of Paclitaxel. Obviously, as the concentration of paclitaxel increases, the survival rate of cells gradually decreases. We choose the gradient of 5 (4 μM) as the paclitaxel concentration of the experimental groups D-F. In groups D-E, Paclitaxel, 1-heptanols and Meclofenamic Acid were used to incubate cells in three different working solutions. They were paclitaxel and 1-heptanols, paclitaxel and Meclofenamic acid, paclitaxel, 1-heptanols and Meclofenamic acid. Among them, the concentration of paclitaxel remained unchanged, but the concentration of 1-H and MA increased gradually. It can be seen that under incubation of high concentration of paclitaxel, the survival rate of cells can be increased by adding gap junction blockers.

Biomedical Optics EXPRESS

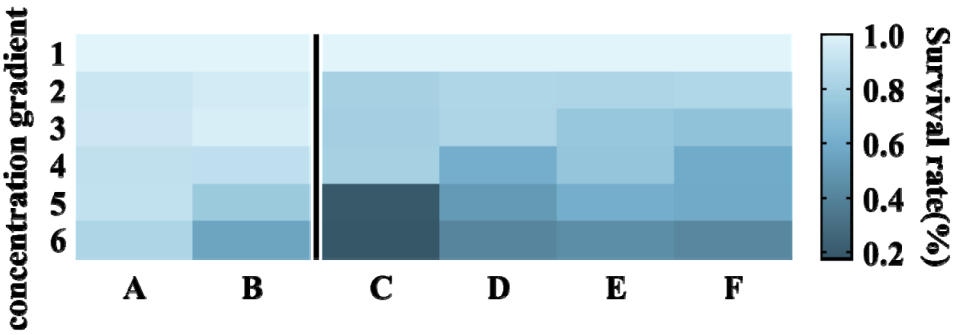

Fig. 5. The CCK-8 result of OVCAR3 cells after treatment with six combinations. A: 1-heptanol; B: Meclofenamic acid; C: Paclitaxel; D: Paclitaxel and 1-heptanol; E: Paclitaxel and Meclofenamic acid; F: Paclitaxel, 1-heptanol and Meclofenamic acid.

To sum up, the results of cck8 showed that the apoptosis rate of OVCAR3 cells was significantly lower than that of the treatment with paclitaxel alone. Collectively, our data demonstrate that TNTs can slow down the rate of cell apoptosis during paclitaxel treatment. Drugs can be preferentially transmitted to adjoining cells through TNTs, which provides a new approach for cancer treatment. Our findings indicate TNTs as a potential novel mechanism in cancer treatment.

4. Conclusion

In this work, we found that there are numerous TNTs-like structures in OVCAR3 cells. A series of fluorescence probes were used to label these TNTs-like structures, which proved to be TNTs. TP-FLIM-FRET was used to image the plasmid transfected cells and fluorescence lifetime was used to signal the transfer of substances in TNTs. Our experimental results demonstrated that TP-FLIM-FRET can be used to image the labeled protein interaction without destroying the structure of TNTs. To study the role of TNTs in cancer treatment, OVCAR3 cells were treated with different concentrations of paclitaxel and gap junction blockers which have been used to regulate the number of TNTs in OVCAR3 cells. The results confirmed that destroying the structure of TNTs can reduce the mortality of cancer cells in drug treatment. Our observations open the possibility of mediate cancer treatment effect by the TNTs processes.

Funding. Shenzhen Technical Project (JCYJ20180305124902165); (Key) Project of Department of Education of Guangdong Province (2016KCXTD007); China Postdoctoral Science Foundation (2018M643159); National Natural Science Foundation of China (61525503, 61835009, 61935012, 61961136005); National Key Research and Development Program of China (2017YFA0700402).

Disclosures. The authors declare that there are no conflicts of interest related to this article.

Supplemental document. See Supplement 1 for supporting content.

References

1. E. Lou, P. O'Hare, S. Subramanian, and C. J. Steer, "Lost in translation: applying 2D intercellular communication via tunneling nanotubes in cell culture to physiologically relevant 3D microenvironments," FEBS J. **284**(5), 699–707 (2017).
2. A. Becker, B. K. Thakur, J. M. Weiss, H. S. Kim, H. Peinado, and D. Lyden, "Extracellular vesicles in cancer: cell-to-cell mediators of metastasis," Cancer Cell **30**(6), 836–848 (2016).
3. R. Kalluri and V. S. LeBleu, "The biology, function, and biomedical applications of exosomes," Science **367**(6478), eaau6977 (2020).
4. X. Chen, H. W. Liang, J. F. Zhang, K. Zen, and C. Y. Zhang, "Secreted microRNAs: a new form of intercellular communication," Trends Cell Biol. **22**(3), 125–132 (2012).
5. D. Landschaft, "Gaps and barriers: Gap junctions as a channel of communication between the soma and the germline," Semin. Cell Dev. Biol. **97**, 167–171 (2020).
6. A. Rustom, R. Saffrich, I. Markovic, P. Walther, and H. H. Gerdes, "Nanotubular highways for intercellular organelle transport," Science **303**(5660), 1007–1010 (2004).

Biomedical Optics EXPRESS

7. Y. Wang, J. Cui, X. Sun, and Y. Zhang, "Tunneling-nanotube development in astrocytes depends on p53 activation," Cell Death Differ **18**(4), 732–742 (2011).
8. K. McCoy-Simandle, S. J. Hanna, and D. Cox, "Exosomes and nanotubes: Control of immune cell communication," Int. J. Biochem. Cell Biol. **71**, 44–54 (2016).
9. M. L. Vignais, A. Caicedo, J. M. Brondello, and C. Jorgensen, "Cell connections by tunneling nanotubes: effects of mitochondrial trafficking on target cell metabolism, homeostasis, and response to therapy," Stem Cells Int. **2017**, 1–14 (2017).
10. V. Thayanithy, E. L. Dickson, C. Steer, S. Subramanian, and E. Lou, "Tumor-stromal cross talk: direct cell-to-cell transfer of oncogenic microRNAs via tunneling nanotubes," Transl Res. **164**(5), 359–365 (2014).
11. J. Hurtig, D. T. Chiu, and B. Onfelt, "Intercellular nanotubes: insights from imaging studies and beyond," WIREs Nanomed. Nanobiotechnol. **2**(3), 260–276 (2010).
12. M. D. Kolba, W. Dudka, M. Zareba-Koziol, A. Kominek, P. Ronchi, L. Turos, P. Chroscicki, J. Wlodarczyk, Y. Schwab, A. Klejman, D. Cysewski, K. Srpan, D. M. Davis, and K. Piwocka, "Tunneling nanotube-mediated intercellular vesicle and protein transfer in the stroma-provided imatinib resistance in chronic myeloid leukemia cells," Cell Death Dis. **10**(11), 817 (2019).
13. W. Becker, "Fluorescence lifetime imaging - techniques and applications," J. Microsc-Oxford **247**(2), 119–136 (2012).
14. C. Thaler, S. V. Koushik, P. S. Blank, and S. S. Vogel, "Quantitative multiphoton spectral imaging and its use for measuring resonance energy transfer," Biophys. J. **89**(4), 2736–2749 (2005).
15. A. D. Elder, A. Domin, G. S. K. Schierle, C. Lindon, J. Pines, A. Esposito, and C. F. Kaminski, "A quantitative protocol for dynamic measurements of protein interactions by Forster resonance energy transfer-sensitized fluorescence emission," J. R. Soc. Interface. **6**(suppl_1), S59–S81 (2009).
16. T. Zal and N. R. Gascoigne, "Photobleaching-corrected FRET efficiency imaging of live cells," Biophys J. **86**(6), 3923–3939 (2004).
17. M. Tramier, I. Gautier, T. Piolot, S. Ravalet, K. Kemnitz, J. Coppey, C. Durieux, V. Mignotte, and M. Coppey-Moisan, "Picosecond-hetero-FRET microscopy to probe protein-protein interactions in live cells," Biophys. J. **83**(6), 3570–3577 (2002).
18. H. Wallrabe and A. Periasamy, "Imaging protein molecules using FRET and FLIM microscopy," Curr. Opin Biotech. **16**(1), 19–27 (2005).
19. S. Desir, P. O'Hare, R. I. Vogel, W. Sperduto, A. Sarkari, E. L. Dickson, P. Wong, A. C. Nelson, Y. Fong, C. J. Steer, S. Subramanian, and E. Lou, "Chemotherapy-induced tunneling nanotubes mediate intercellular drug efflux in pancreatic cancer," Sci. Rep. **8**(1), 9484 (2018).
20. A. Kretschmer, F. Zhang, S. P. Somasekharan, C. Tse, L. Leachman, A. Gleave, B. Li, I. Asmaro, T. Huang, L. Kotula, P. H. Sorensen, and M. E. Gleave, "Stress-induced tunneling nanotubes support treatment adaptation in prostate cancer," Sci. Rep. **9**(1), 7826 (2019).
21. B. Shen, S. Wang, G. Bharathi, Y. Li, F. Lin, R. Hu, L. Liu, and J. Qu, "Rapid and targeted photoactivation of $Ca^{(2+)}$ channels mediated by squaraine to regulate intracellular and intercellular signaling processes," Anal. Chem. **92**(12), 8497–8505 (2020).
22. D. M. Davis and S. Sowinski, "Membrane nanotubes: dynamic long-distance connections between animal cells," Nat. Rev. Mol. Cell Biol. **9**(6), 431–436 (2008).
23. S. Sowinski, C. Jolly, O. Berninghausen, M. A. Purbhoo, A. Chauveau, K. Kohler, S. Oddos, P. Eissmann, F. M. Brodsky, C. Hopkins, B. Onfelt, Q. Sattentau, and D. M. Davis, "Membrane nanotubes physically connect T cells over long distances presenting a novel route for HIV-1 transmission," Nat. Cell Biol. **10**(2), 211–219 (2008).
24. S. Gurke, J. F. V. Barroso, and H. H. Gerdes, "The art of cellular communication: tunneling nanotubes bridge the divide," Histochem. Cell Biol. **129**(5), 539–550 (2008).
25. A. Sartori-Rupp, D. Cordero Cervantes, A. Pepe, K. Gousset, E. Delage, S. Corroyer-Dulmont, C. Schmitt, J. Krijnse-Locker, and C. Zurzolo, "Correlative cryo-electron microscopy reveals the structure of TNTs in neuronal cells," Nat. Commun. **10**(1), 342 (2019).
26. H. X. Yang, T. K. Borg, Z. Ma, M. F. Xu, G. Wetzel, L. V. Saraf, R. Markwald, R. B. Runyan, and B. Z. Gao, "Biochip-based study of unidirectional mitochondrial transfer from stem cells to myocytes via tunneling nanotubes," Biofabrication **8**(1), 015012 (2016).
27. R. J. J. Jansens, A. Tishchenko, and H. W. Favoreel, "Bridging the gap: virus long-distance spread via tunneling nanotubes," J. Virol. **94**(8), e02120-19 (2020).
28. E. A. Jares-Erijman and T. M. Jovin, "FRET imaging," Nat. Biotechnol. **21**(11), 1387–1395 (2003).
29. A. Miyawaki, J. Llopis, R. Heim, J. M. McCaffery, J. A. Adams, M. Ikura, and R. Y. Tsien, "Fluorescent indicators for Ca^{2+} based on green fluorescent proteins and calmodulin," Nature **388**(6645), 882–887 (1997).
30. Y. Chen and A. Periasamy, "Characterization of two-photon excitation fluorescence lifetime imaging microscopy for protein localization," Microsc. Res. Tech. **63**(1), 72–80 (2004).
31. E. Gratton, S. Breusegem, J. Sutin, and Q. Q. Ruan, "Fluorescence lifetime imaging for the two-photon microscope: time-domain and frequency-domain methods," J. Biomed. Opt. **8**(3), 381–390 (2003).
32. N. M. Kumar and N. B. Gilula, "The gap junction communication channel," Cell **84**(3), 381–388 (1996).

Biomedical Optics EXPRESS

33. X. Wang, M. L. Veruki, N. V. Bukoreshtliev, E. Hartveit, and H. H. Gerdes, "Animal cells connected by nanotubes can be electrically coupled through interposed gap-junction channels," Proc. Natl. Acad. Sci. U. S. A. **107**(40), 17194–17199 (2010).
34. D. Gonzalez, J. M. Gomez-Hernandez, and L. C. Barrio, "Molecular basis of voltage dependence of connexin channels: An integrative appraisal," Prog. Biophys. Mol. Biol. **94**(1-2), 66–106 (2007).
35. X. Wang and H. H. Gerdes, "Long-distance electrical coupling via tunneling nanotubes," Biochim. Biophys. Acta **1818**(8), 2082–2086 (2012).
36. A. Rustom, "The missing link: does tunnelling nanotube-based supercellularity provide a new understanding of chronic and lifestyle diseases?" Open Biol. **6**(6), 160057 (2016).
37. S. Sisakhtnezhad and L. Khosravi, "Emerging physiological and pathological implications of tunneling nanotubes formation between cells," Eur. J. Cell Biol. **94**(10), 429–443 (2015).
38. M. Omsland, C. Pise-Masison, D. Fujikawa, V. Galli, C. Fenizia, R. W. Parks, B. T. Gjertsen, G. Franchini, and V. Andresen, "Inhibition of Tunneling Nanotube (TNT) Formation and Human T-cell Leukemia Virus Type 1 (HTLV-1) Transmission by Cytarabine," Sci. Rep. **8**(1), 11118 (2018).
39. S. K. Nirala, M. Bhadauria, R. Mathur, P. Q. Li, and G. Q. Guo, "Intercellular Communication through Tunneling Nanotubes: A Possible Target for Anti-Cancer Therapies," J. Hepatol. **50**, S197 (2009).
40. J. Ady, V. Thayanithy, K. Mojica, P. Wong, J. Carson, P. Rao, Y. M. Fong, and E. Lou, "Tunneling nanotubes: an alternate route for propagation of the bystander effect following oncolytic viral infection," Mol. Ther-Oncolytics **3**, 16029 (2016).
41. R. J. J. Jansens, W. Van den Broeck, S. De Pelsmaeker, J. A. S. Lamote, C. Van Waesberghe, L. Couck, and H. W. Favoreel, "Pseudorabies virus US3-induced tunneling nanotubes contain stabilized microtubules, interact with neighboring cells via cadherins, and allow intercellular molecular communication," J. Virol. **91**(19), e00749-17 (2017).
42. A. Burtey, M. Wagner, E. Hodneland, K. O. Skaftnesmo, J. Schoelermann, I. R. Mondragon, H. Espedal, A. Golebiewska, S. P. Niclou, R. Bjerkvig, T. Kogel, and H. H. Gerdes, "Intercellular transfer of transferrin receptor by a contact-, Rab8-dependent mechanism involving tunneling nanotubes," FASEB J. **29**(11), 4695–4712 (2015).
43. S. Abounit, J. W. Wu, K. Duff, G. S. Victoria, and C. Zurzolo, "Tunneling nanotubes: A possible highway in the spreading of tau and other prion-like proteins in neurodegenerative diseases," Prion **10**(5), 344–351 (2016).
44. M. Omsland, V. Andresen, S. E. Gullaksen, P. Ayuda-Duran, M. Popa, R. Hovland, A. Brendehaug, J. Enserink, E. McCormack, and B. T. Gjertsen, "Tyrosine kinase inhibitors and interferon-alpha increase tunneling nanotube (TNT) formation and cell adhesion in chronic myeloid leukemia (CML) cell lines," FASEB J. **34**(3), 3773–3791 (2020).
45. J. T. Fong, R. M. Kells, A. M. Gumpert, J. Y. Marzillier, M. W. Davidson, and M. M. Falk, "Internalized gap junctions are degraded by autophagy," Autophagy **8**(5), 794–811 (2012).